PHYSICAL METALLURGY RESEARCH LABORATORIES

REPORT ERP/PMRL 81-19 (TR)

EVALUATION OF THE HAZ TOUGHNESS OF PIPE AE SEAM WELD

by

J.T. McGrath

ABSTRACT

The toughness of the heat-affected-zone (HAZ) of the seam weld of pipe AE was measured using the instrumented impact test. It was found that the yield load fracture transition temperature of the HAZ was 45°C higher than that of the neighbouring base metal.

The decrease in toughness is attributed to a coarse bainitic microstructure in the HAZ.

INTRODUCTION

In the evaluation of Arctic grade line pipe in the CANMET project "Evaluation of Materials for Natural Gas Pipeline", the structure and mechanical properties of base metal, weld metal and heat-affected-zone are being measured.

The objective of this study was to evaluate the notch toughness of the heat-affected-zone of the seam weld of a grade 483 Arctic grade line pipe designated pipe AE.

EXPERIMENTAL PROCEDURE

The heat-affected-zone (HAZ) toughness of the mill seam weld of pipe AE was measured. Pipe AE which has a diameter of 1219 mm and a wall thickness of 13.7 mm had been mechanically expanded to final size. The chemistry of the steel is listed in Table 1. The mill seam weld was produced by submerged-arc-welding with an average energy input of 3 KJ/mm resulting in a cooling rate in the coarse-grained heat-affected-zone (CGHAZ) of $\Delta t_{800°C-500°C} \simeq 27s$.

The notch toughness of the CGHAZ was determined by the instrumented impact test. The toughness of the base metal was also assessed for comparison purposes. Full-size Charpy specimens (10x10 mm) were prepared from the seam weld with the long axis of the specimens perpendicular to the weld centre line. The weld centre line is also parallel to the plate rolling direction. Specimens prepared from the base metal had a similar orientation, i.e., the long axis was perpendicular to the rolling direction. The specimens were machine-notched from the outside surface to a depth of 1.5 mm. The tip of the notch was extended to about 3 mm by fatigue. In the case of the HAZ specimens the tip of the fatigue crack was located in the CGHAZ. Details of the instrumented impact test technique are included elsewhere (1). The notch toughness evaluation was done over a temperature range of -75° to 100°C with at least 3 specimens tested at each temperature.

The microstructures of the base metal and HAZ region were examined by optical metallography.

RESULTS

NOTCH TOUGHNESS

The fracture loads obtained from the instrumented impact tests are listed in Tables 2 and 3 for the CGHAZ and the base metal, respectively. In the case of the HAZ, fracture initiation loads were less than the yield load for test temperatures <25°C. Some post-yield deformation prior to abrupt fracture initiation was observed at 50°C, while maximum load ductile fracture occurred only at 100°C. Typical load/time plots for these 3 temperature regimes are shown in Fig. 1.

As shown in Table 3 pre-yield fracture initiation occurred in the base metal at temperatures <-25°C. Post-yield abrupt fracture was found at 25°C and maximum load ductile fracture took place at temperatures >50°C.

The values of yield, maximum and fracture loads were used to calculate the relevant stress intensities K_Y, K_M and K_F using Equation 1 (2).

$$K = \frac{P.\ S.}{B.W^{3/2}} \cdot f(a/_W) \qquad (1)$$

where $f(a/_W) = 3(a/_W)^{1/2} \dfrac{[1.99-(a/_W)(1-a/_W)(2.15-3.93a/_W+2.7a^2/_W^2)]}{2(1+2a/W)\ (1-a/W)^{3/2}}$

P = load, KN

B = specimen thickness, cm

S = span, cm

W = specimen depth, cm

a = crack length, cm.

The values of stress intensity are plotted against temperature in Fig. 2 and 3. The yield load fracture transition temperature, T_F, was used to define the level of notch toughness. The fracture transition temperature for the CGHAZ of steel AE was about 45°C higher than that of the base metal.

MICROSTRUCTURE

Base Metal

The controlled rolled base metal microstructure was composed of layers of polygonal ferrite grains (grain size, 10-20 μm) and fine grains of the order of 3-5μm in diameter as shown in Fig. 4. Godden has identified the fine grain structure in steel AE as predominantly martensite-austenite (3). The M-A regions contain fine martensite microtwins.

The fracture surface features reflected the mode of fracture in the base metal. In the temperature range from 25° to 100°C where plastic deformation preceded final fracture, splitting was observed on the fracture surface with the direction of the splits being parallel to the rolling plane as shown in Fig. 5a. When a completely brittle fracture occurred at -75°C, cleavage facets replaced the splitting phenomenon and the fracture profile was at an angle of 40° to the plate surface as shown in Fig. 5b.

HAZ

The CGHAZ Region was about 1 mm wide with an average grain size of 100μm. The structure was predominantly coarse bainite as shown in Fig. 6. The bainite consisted of ferrite laths with a light etching constituent between the laths. This constituent is likely martensite-austenite. Godden analysed the HAZ microstructures of AE pipe welds by transmission electron microscopy and verified the presence of fine martensite microtwins between the ferrite laths (3).

Examination of the fractured surfaces of the HAZ specimens revealed cleavage facets within the HAZ in all specimens fractured at temperatures $\leq$50°C.

DISCUSSION

It has been shown that the notch toughness associated with fracture initiation is significantly lower in the CGHAZ of the seam weld of pipe AE than in the neighbouring base metal. The difference in toughness can be related to microstructure. In terms of grain size, the average grain diameter in the base metal, despite the banded nature of the grain structure, was much finer than that of the CGHAZ. It is well known that the coarse bainite structure of the HAZ does not have a high resistance to fracture initiation

and propagation (4). In addition to the coarse grain structure of the HAZ another factor which reduces the fracture toughness is the presence of the martensite-austenite constituent along ferrite lath boundaries as shown in Fig. 6. These elongated film-like M-A regions contained twinned martensite and should not offer much resistance to crack initiation and propagation within the CGHAZ. The presence of martensite-austenite regions is not uncommon in weldments of HSLA steels. The conditions which determine its formation are composition and cooling rate (5). No attempt will be made to analyse M-A formation in steel AE at this time.

A secondary effect, i.e., the formation of splits during fracture of AE base metal, should be addressed. Splitting on fracture faces of controlled-rolled HSLA steels has been observed previously (6). As reviewed by Speich and Dabkowski, splitting is almost always associated with the presence of intense banding of coarse and fine grain structures (6). The bands or sheets are parallel to the rolling plane. It was suggested that splitting occurred by formation of brittle cleavage cracks in the coarse grained regions aligned parallel to the rolling plane followed by tearing of the fine-grained regions between them. Splitting can be eliminated by removing the banded microstructure by such heat treatment operations as normalizing or quenching and tempering. Furthermore, it was suggested that severe banding in controlled-rolled steels can be avoided by using higher finishing temperatures in the controlled-rolling schedule where austenite and only a minimal amount of ferrite are present (6).

CONCLUSIONS

1. The notch toughness of the coarse-grained heat-affected-zone region of the mill seam weld of pipe AE was evaluated using the instrumented impact test.
2. The toughness of the CGHAZ was significantly less than that of the base metal. For example, the fracture load transition temperature was about 45°C higher for the CGHAZ in comparison with the base metal.
3. The lower toughness of the CGHAZ can be attributed to a coarse-grained bainitic microstructure that contained regions of an embrittling martensite-austenite constituent.

ACKNOWLEDGEMENTS

The author wishes to thank Mr. R. Narraway for his assistance in all phases of the experimental program. He also thanks Mr. G. Weatherall for performing the instrumented impact tests.

REFERENCE

1. McGrath, J.T., Godden, M.G., Gordine, J. and Boyd, J.D.; Can. Met. Quart. 19, 99; 1980.

2. ASTM, Plane Strain Fracture Toughness of Metallic Materials, E 399-78a, 1980.

3. Godden, M.J.; Division Report ERP/PMRL 80-84(TR), CANMET, Energy, Mines and Resources Canada; 1980.

4. Taylor, L.G. and Farrar R.A.; Welding and Met. Fab. 43, 305; 1975.

5. Glover, A.G., McGrath, J.T., Tinkler, M.J. and Weatherly, G.C.; Welding J. 56, No. 9, 267-S; 1977.

6. Speich, G.R. and Dabkowski D.S.; "The hot deformation of austenite"; Proc. AIME Conf., Cleveland, p 557; 1979.

Table 1. Composition of steel AE

C	S	P	Si	Mn	Ni	Cr	Mo	V	Nb	Cu
0.08	0.005	0.011	0.29	1.98	0.033	0.097	0.24	0.05	0.045	0.053

Table 2. Instrumented impact results for the CGHAZ of steel AE

Specimen	Temp. °C	a cm	P_Y KN	P_M KN	P_F KN	K_Y MPa$\sqrt{m}$	K_M MPa$\sqrt{m}$	K_F MPa$\sqrt{m}$
2	25	0.349			9.8			67.7
4	25	0.334			8.2			54.6
5	25	0.336			6.7			44.6
6	25	0.354			8.7			60.7
7	-25	0.329			10.9			71.5
8	-25	0.349			8.0			55.4
9	-25	0.342			8.0			54.4
10	-50	0.315			5.8			36.5
12	-50	0.345			6.0			41.1
22	-50	0.396			6.7			52.6
30	-75	0.354			4.5			31.1
31	-75	0.310			5.1			32.1
34	-75	0.307			4.9			30.5
32	50	0.352	10.0		11.1	69.7		77.4
42	50	0.348			7.8			32.4
44	50	0.385	8.7		10.9	66.3		83.3
36	100	0.311	10.9	14.7		68.4	92.2	
38	100	0.390	8.9	11.8		68.7	91.0	
39	100	0.337	9.3	13.6		62.4	90.6	

Table 3. Instrumented impact results for steel AE base metal

Specimen	Temp. °C	a cm	P_Y KN	P_M KN	P_F KN	K_Y MPa$\sqrt{m}$	K_M MPa$\sqrt{m}$	K_F MPa$\sqrt{m}$
1	25	0.329	8.9		10.7	67.6		81.1
2	25	0.304	9.8		13.3	60.3		82.2
3	25	0.367	8.5		10.9	58.3		79.3
4	-25	0.365			8.9			64.1
5	-25	0.407			6.9			56.0
7	-25	0.406			6.5			52.1
6	-50	0.358			6.9			48.8
8	-50	0.335			6.9			46.1
9	-50	0.353			6.5			45.2
10	-75	0.342			5.6			37.8
11	-75	0.340			5.3			36.1
12	-75	0.366			5.3			38.6
13	50	0.338	8.5		12.0	56.8		80.7
14	50	0.331	8.7	12.5		57.2	82.2	
16	50	0.337	8.9	12.2		63.2	78.6	
17	100	0.412	7.6	9.6		59.4	81.7	
18	100	0.395	8.5	9.8		62.3	78.8	
15	100	0.387	8.2	10.2		62.8	76.7	

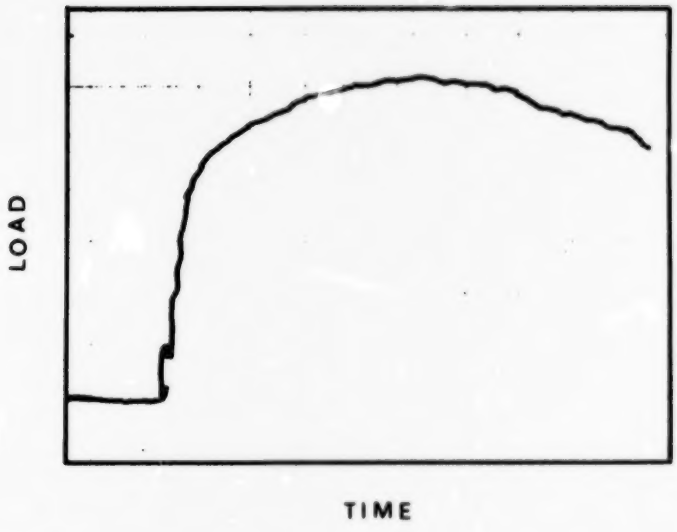

Fig. 1(a). Load/time plot exhibiting maximum load ductile fracture. (neg 4560)

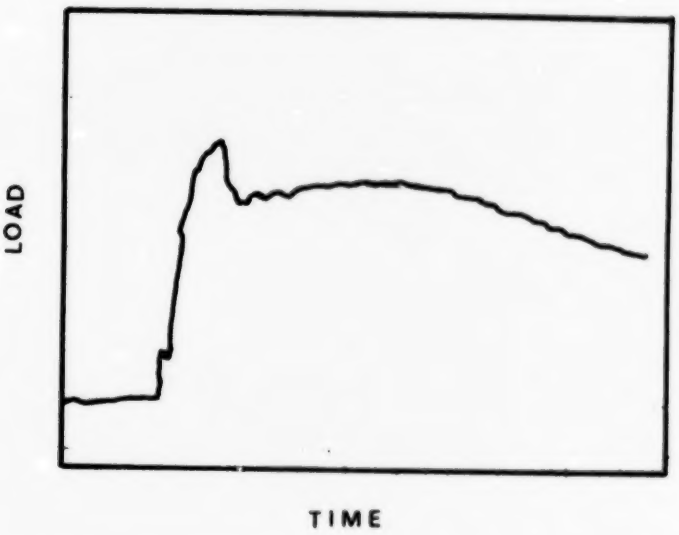

Fig. 1(b). Load/time plot exhibiting post-yield deformation and abrupt fracture. (neg 4562)

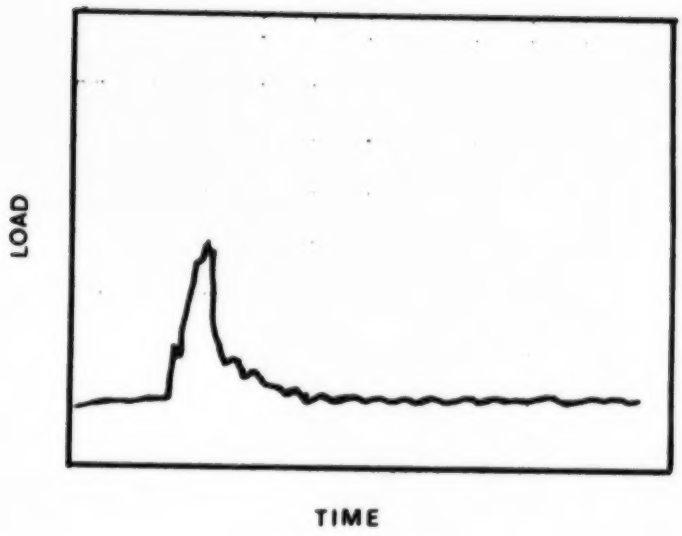

Fig. 1(c). Load/time plot for pre-yield cleavage fracture. (neg 4561)

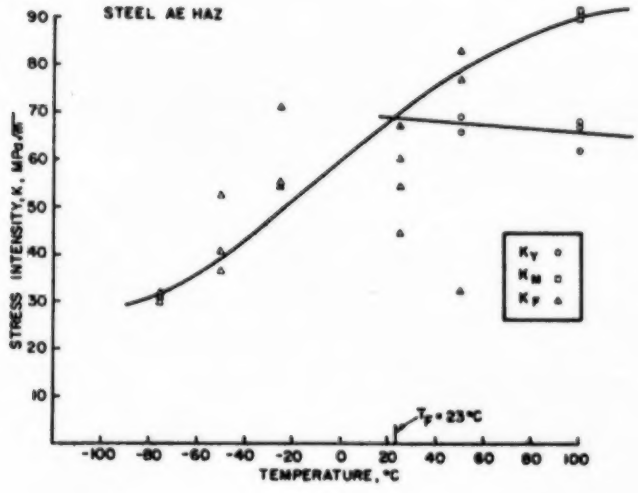

Fig. 2. Stress intensity K versus temperature for CGHAZ of pipe weld AE tested under impact loading. (neg 4734)

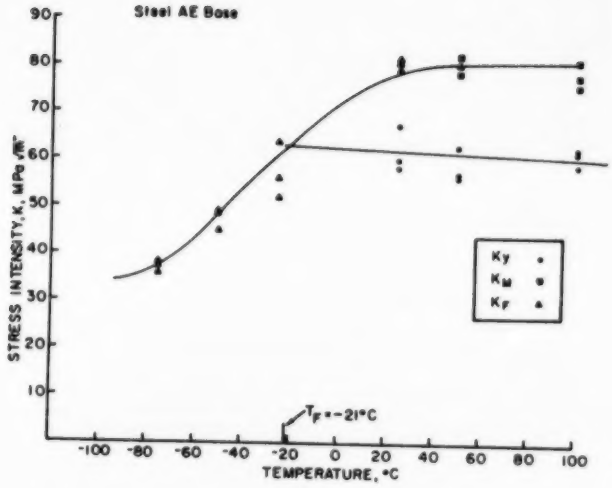

Fig. 3. Stress intensity K versus temperature for base metal of pipe AE tested under impact loading. (neg 4735)

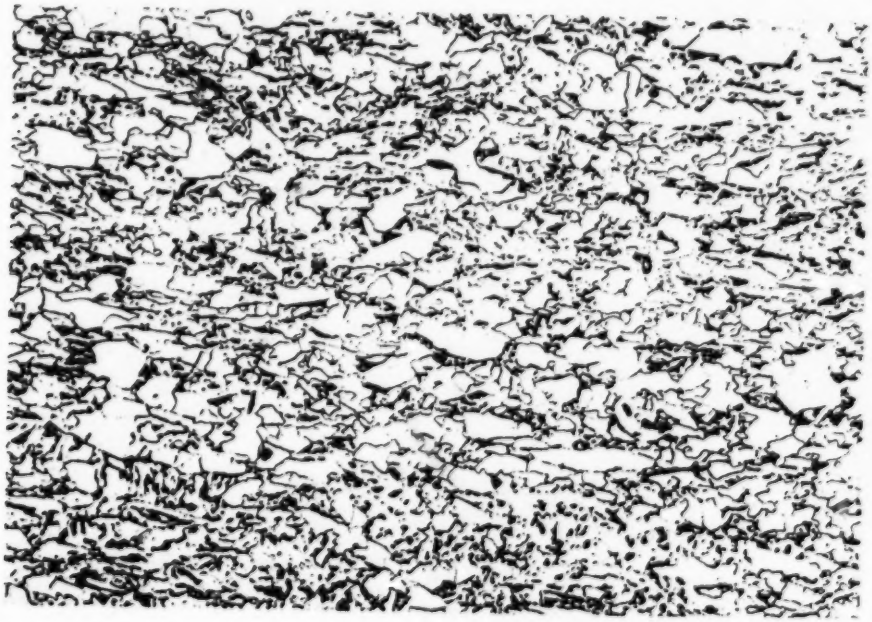

Fig. 4. Controlled rolled base metal microstructure of pipe AE. X500 (neg 7128)

Fig. 5(a). Fracture surface of base metal following ductile fracture under impact loading. X4 (neg 7127)

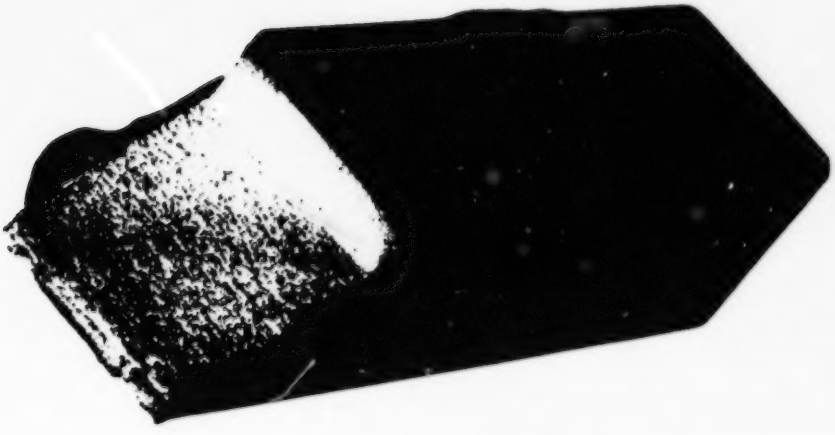

Fig. 5(b). Fracture surface of base metal following brittle cleavage failure under impact loading. X4 (neg 7126)

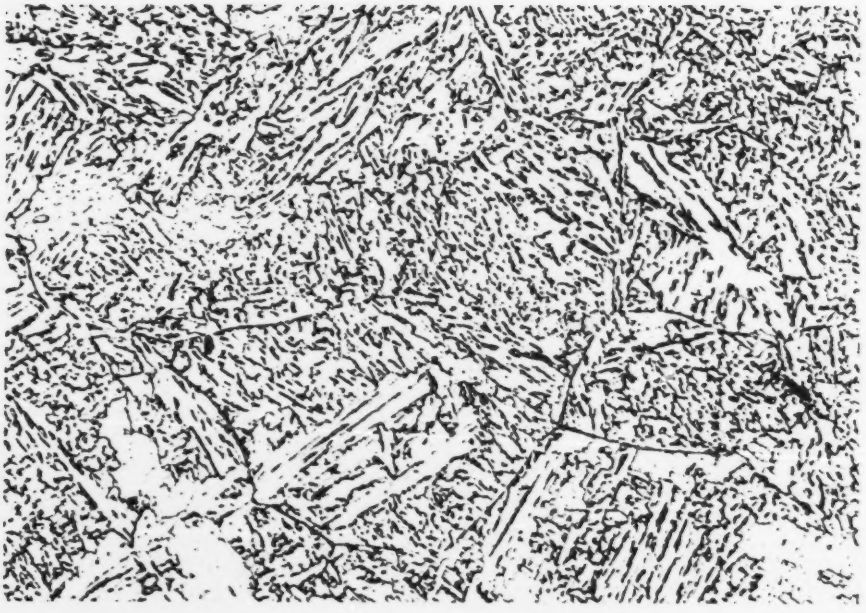

Fig. 6. Coarse grain heat affected zone microstructure of AE seam weld. X500 (neg 7125)